ORIGINAL ARTICLE

Membrane-anchored Serine Protease Matriptase Is a Trigger of Pulmonary Fibrogenesis

Olivier Bardou[1,2*], Awen Menou[1,2*], Charlène François[1,2], Jan Willem Duitman[3], Jan H. von der Thüsen[4], Raphaël Borie[2,5], Katiuchia Uzzun Sales[6,7], Kathrin Mutze[8], Yves Castier[9], Edouard Sage[10], Ligong Liu[11], Thomas H. Bugge[6], David P. Fairlie[11], Mélanie Königshoff[8], Bruno Crestani[1,2,5‡], and Keren S. Borensztajn[1,2‡]

[1]Inserm UMR1152, Medical School Xavier Bichat, Paris, France; [2]Université Paris Diderot, Sorbonne Paris Cité, Département Hospitalo-universitaire FIRE (Fibrosis, Inflammation and Remodeling) and LabEx Inflamex, Paris, France; [3]Center for Experimental and Molecular Medicine, Academic Medical Center, Amsterdam, the Netherlands; [4]Department of Pathology, Erasmus Medical Centre, Rotterdam, the Netherlands; [5]Assistance Publique-Hôpitaux de Paris, Department of Pulmonology A, Competence Center for Rare Lung Diseases, Bichat-Claude Bernard University Hospital, Paris, France; [6]Oral and Pharyngeal Cancer Branch, National Institute of Dental and Craniofacial Research, National Institutes of Health, Bethesda, Maryland; [7]Department of Cell and Molecular Biology, Ribeirão Preto School of Medicine, University of São Paulo Ribeirão Preto, São Paulo, Brazil; [8]Member of the German Center of Lung Research, Comprehensive Pneumology Center, University Hospital, Ludwig-Maximilians University, Helmholtz Zentrum München, Munich, Germany; [9]Assistance Publique-Hôpitaux de Paris, Department of Vascular and Thoracic Surgery, Bichat-Claude Bernard University Hospital, Denis Diderot University and Medical School Paris VII, France; [10]Department of Thoracic Surgery and Lung Transplantation, Hôpital Foch, Suresnes, France; and [11]Institute for Molecular Bioscience, University of Queensland, Brisbane, Queensland, Australia

Abstract

Rationale: Idiopathic pulmonary fibrosis (IPF) is a devastating disease that remains refractory to current therapies.

Objectives: To characterize the expression and activity of the membrane-anchored serine protease matriptase in IPF in humans and unravel its potential role in human and experimental pulmonary fibrogenesis.

Methods: Matriptase expression was assessed in tissue specimens from patients with IPF versus control subjects using quantitative reverse transcriptase–polymerase chain reaction, immunohistochemistry, and Western blotting, while matriptase activity was monitored by fluorogenic substrate cleavage. Matriptase-induced fibroproliferative responses and the receptor involved were characterized in human primary pulmonary fibroblasts by Western blot, viability, and migration assays. In the murine model of bleomycin-induced pulmonary fibrosis, the consequences of matriptase depletion, either by using the pharmacological inhibitor camostat mesilate (CM), or by genetic down-regulation using matriptase hypomorphic mice, were characterized by quantification of secreted collagen and immunostainings.

Measurements and Main Results: Matriptase expression and activity were up-regulated in IPF and bleomycin-induced pulmonary fibrosis. In cultured human pulmonary fibroblasts, matriptase expression was significantly induced by transforming growth factor-β. Furthermore, matriptase elicited signaling via protease-activated receptor-2 (PAR-2), and promoted fibroblast activation, proliferation, and migration. In the experimental bleomycin model, matriptase depletion, by the pharmacological inhibitor CM or by genetic down-regulation, diminished lung injury, collagen production, and transforming growth factor-β expression and signaling.

Conclusions: These results implicate increased matriptase expression and activity in the pathogenesis of pulmonary fibrosis in human IPF and in an experimental mouse model. Overall, targeting matriptase, or treatment by CM, which is already in clinical use for other diseases, may represent potential therapies for IPF.

Keywords: idiopathic pulmonary fibrosis; fibroblast; matriptase; protease-activated receptor-2; camostat mesilate

(Received in original form February 12, 2015; accepted in final form November 17, 2015)

*These authors contributed equally to this work.

‡These authors contributed equally to this work.

Supported by grants from the Fondation pour la Recherche Medicale grant AJE201121 (K.S.B.) and Agence Nationale pour la Recherche ANR-14-CE15-0010-01 (O.B., A.M., and K.S.B.); Dutch Lung Foundation grant 9.2.14.085FE (J.W.D.); the Helmholtz Association (K.M. and M.K.); National Health and Medical Research Council grant 1047759 (L.L. and D.P.F.); Senior Principal Research Fellowship 1027369 (D.P.F.); and the National Institute of Dental and Craniofacial Research Intramural Research Program (T.H.B. and K.U.S.).

Author Contributions: Conception and design: O.B., A.M., K.S.B., and B.C.; analysis and interpretation: C.F., A.M., J.W.D., J.H.v.d.T., R.B., K.U.S., K.M., E.S., Y.C., L.L., T.H.B., D.P.F., and M.K.; drafting the manuscript for important intellectual content: O.B., A.M., K.S.B., and B.C.

Correspondence and requests for reprints should be addressed to Keren S. Borensztajn, Ph.D., INSERM UMR1152, Faculté de médecine Xavier Bichat, 16 rue Henri Huchard, 75018 Paris, France. E-mail: keren.borensztajn@inserm.fr

This article has an online supplement, which is accessible from this issue's table of contents at www.atsjournals.org

Am J Respir Crit Care Med Vol 193, Iss 8, pp 847–860, Apr 15, 2016

Originally Published in Press as DOI: 10.1164/rccm.201502-0299OC on November 24, 2015
Internet address: www.atsjournals.org

At a Glance Commentary

Scientific Knowledge on the Subject: Idiopathic pulmonary fibrosis (IPF) is characterized by the deposition of excessive extracellular matrix and the destruction of lung parenchyma, resulting from an aberrant wound-healing response. Although IPF is often associated with an imbalance in protease activity, the mechanisms underlying the sustained repair mechanisms are not fully understood.

What This Study Adds to the Field: We showed that the recently identified membrane-anchored serine protease matriptase is up-regulated in IPF in humans and during pulmonary fibrogenesis in mice. Matriptase triggers fibroproliferative responses in pulmonary cells via protease-activated receptor-2 activation. In an experimental mouse model, lung injury and fibrosis were reduced through matriptase depletion, using either the pharmacological inhibitor camostat mesilate (already in clinical use for other diseases) or by genetic down-regulation by using matriptase hypomorphic mice, which have a 93% reduction in lung matriptase mRNA levels. These data indicate that matriptase is influential in promoting pulmonary fibrogenesis *in vivo* and show that camostat mesilate is a potential treatment for IPF.

Idiopathic pulmonary fibrosis (IPF) is a devastating chronic fibrotic lung disease with a median survival of 2 to 3 years (1). Options for the treatment of IPF are limited. Only two drugs, pirfenidone and nintedanib, have demonstrated efficacy in slowing fibrosis progression in patients with mild to moderate IPF (2, 3). Therefore, novel treatment options are sorely needed. The current paradigm on the underlying pathogenic mechanisms postulates that IPF is an "epithelial-fibroblastic disease" (i.e., a fibroproliferative disorder preceded by alveolar epithelial injury and activation, with fibrotic foci representing the primary sites of injury and aberrant repair) (1). The precise signals triggering the aberrant and sustained wound healing response in IPF remain elusive and represent an area of intense investigation. Evidence for diffuse infiltration of immune cells in the fibrotic lung also strongly suggest that autoimmunity plays a role in the course of the disease. Accordingly, immunomodulatory therapies are currently being evaluated in early-phase clinical trials (4, 5).

Matriptase belongs to the recently identified type II transmembrane serine protease family (6). Membrane anchorage enables matriptase to initiate pericellular proteolysis in the microenvironment and to interact with vicinal membrane proteins on the same cell surface and/or on neighboring cells. Matriptase activity is regulated by hepatocyte growth factor activator inhibitor (HAI) type 1, through formation of a stoichiometric 1:1 complex. Over the last decade, compelling evidence has demonstrated that matriptase deregulation is influential in a broad variety of pathological processes, including cancer and skin diseases (6, 7). Three major macromolecular substrates of matriptase have been identified: hepatocyte growth factor, protease-activated receptor 2 (PAR-2), and urokinase-type plasminogen activator (6). Through the cleavage of these substrates, matriptase triggers specific responses, including cell proliferation, migration, inflammatory cytokine production, inflammatory cell recruitment, hyperplasia, and fibrosis (8, 9). These responses are crucial in fibrotic diseases (10, 11), but the role of matriptase in fibrotic disorders has thus far never been explored.

We recently established a link between PAR-2 and pulmonary fibrosis progression in humans and mice (12). PAR-2 belongs to the G-protein-coupled receptor superfamily. Its activation by proteolytic cleavage triggers multiple cell-signaling pathways, the functional consequences of which are crucial in pathologies such as aberrant wound repair mechanisms (13). However, the relevant PAR-2 agonists involved in IPF remain unknown. Considering that matriptase is expressed physiologically in murine and human lung (14), orchestrates tissue remodelling through its potent trypsin-like activity, and is able to activate PAR-2, in the present study we explore whether matriptase is implicated in the progression of human and experimental pulmonary fibrosis.

Methods

Methodology for the murine bleomycin model, collagen quantification, quantitative reverse transcriptase–polymerase chain reaction (qRT-PCR), cell culture studies, histology, and immunohistochemistry can be found in the online supplement.

Human Tissues

Lung tissue was obtained from 61 patients with IPF (8 women, 53 men; mean age, 57.6 ± 7.5 yr), and 43 control subjects (patients undergoing lung surgery for removal of a primary lung tumor; mean age, 62.5 ± 13.8 yr; 17 women, 26 men). Control tissues were obtained from a noninvolved segment, remote from the solitary tumor lesion, and normalcy of

Table 1. Matriptase and HAI-1 mRNA Levels in Normal and Affected Tissues

	mRNA Levels in n = 22 Control Tissues	mRNA Levels in n = 29 IPF Tissues
Matriptase	0.0074 (0.0007)	0.011 (0.001), $P = 0.0024$
HAI-1	0.093 (0.006)	0.12 (0.01), $P = 0.0418$
Ratio matriptase/HAI-1	0.08 (0.006)	0.099 (0.007), $P = 0.046$

Definition of abbreviations: HAI-1 = hepatocyte growth factor activator inhibitor type 1; IPF = idiopathic pulmonary fibrosis.
Data presented as mean (SEM). The mRNA levels were normalized to ubiquitin mRNA levels. *P* value for the comparison of the expression levels in control and IPF tissues.

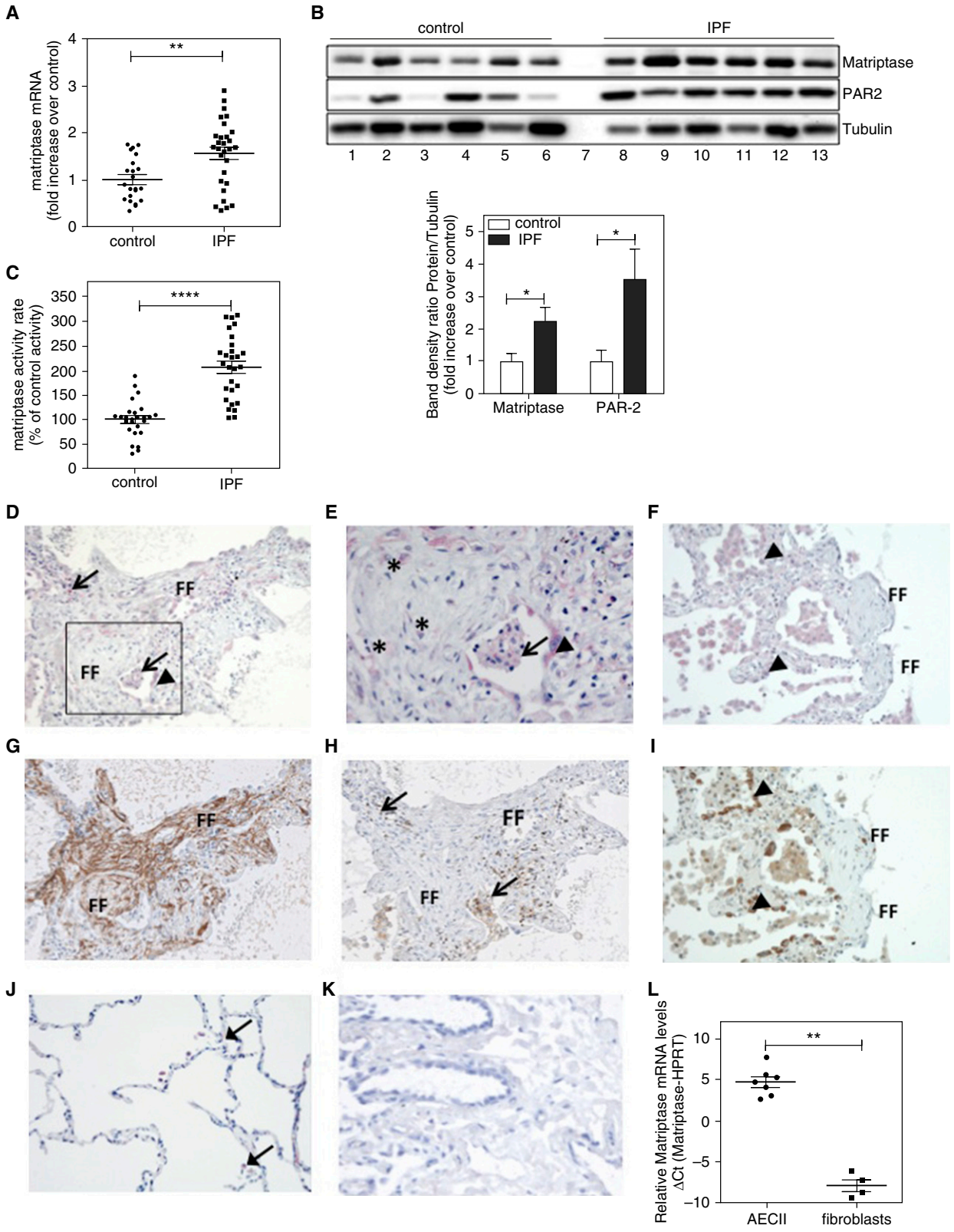

Figure 1. Matriptase expression and activity are up-regulated in the lungs of patients with idiopathic pulmonary fibrosis (IPF) compared with control subjects. (*A*) Scatter dot plot representation of the mRNA levels of matriptase assessed in control (n = 22) and IPF (n = 29) lung specimens by quantitative reverse transcriptase–polymerase chain reaction and normalized to ubiquitin expression. Results represent the mean fold increase over control ± SEM. $^{**}P < 0.01$. (*B*) (*Top*) Immunoblot analysis of matriptase and protease-activated receptor-2 (PAR-2) expression in lung homogenate of control subjects

control lungs was verified histologically as described previously (15, 16). Primary fibroblasts were isolated as described in Reference 15. The study protocol was approved by the institutional ethics committee (Comité d'éthique du CEERB Paris Nord, biobank registration number DC 2009-940). Details for isolation of alveolar type II cells (AECs) and fibroblasts from the German cohort are provided in the Methods section in the online supplementary.

Animals

C57BL/6N mice were from Janvier Labs (Le Genest Saint Isle, France). When indicated, 0.5 mg camostat mesilate (CM) treatment was initiated 7 days after bleomycin challenge. CM was administrated intranasally every other day from Days 7 to 14. Matriptase hypomorphic mice have been described previously (17). Briefly, these mice possess one null allele and one allele in which a reporter gene trap is inserted into the matriptase locus and disrupts gene expression. A low level of alternative splicing in the gene trap allele results in low-level synthesis of full-length matriptase, which is sufficient to enable mouse survival. Experiments with matriptase hypomorphic mice were littermate controlled from mice generated from heterozygous crosses (18). The bleomycin murine model of pulmonary fibrosis was set up as described previously (19). Additional details are provided in the online supplement.

Statistical Analyses

Statistical analyses were conducted using GraphPad Prism (GraphPad Software, San Diego, CA). Data are expressed as mean ± SEM. Comparisons between two groups were analyzed using two-tailed unpaired *t* tests when the data were normally distributed; otherwise Mann-Whitney analysis was performed. *P* values less than 0.05 were considered to indicate a statistically significant difference.

Results

Increased Matriptase Expression and Activity in the Lungs of Patients with IPF

We first investigated whether the expression and activity of matriptase are deregulated in IPF. The mRNA levels of matriptase were determined in human lung tissue specimens from control subjects and patients with IPF using qRT-PCR. As shown in Table 1 and Figure 1A, in IPF tissues, matriptase mRNA was significantly up-regulated (by 1.6 ± 0.1-fold) compared with control. We confirmed matriptase up-regulation by immunoblotting. As shown in Figure 1B, in control lungs (*lanes 1–6*), matriptase expression is low, and it increased by 2.25-fold in IPF lungs (*lanes 8–12*). Additionally, consistent with previous studies (20, 21), PAR-2 expression was up-regulated in IPF lung (3.5 ± 2-fold) (Figure 1B). Subsequently, we determined the proteolytic activity of matriptase in control and IPF tissues by monitoring the cleavage of its highly specific fluorogenic peptide substrate t-butyloxycarbonyl Boc-Gln-Ala-Arg-MCA (Boc-QAR-AMC) (7, 22). Figure 1C shows that the proteolytic activity significantly increased (206 ± 65%) in IPF lungs compared with control lungs. Consistently, increased matriptase antigen level and activity were detected in bronchoalveolar lavage fluid of patients with IPF (*see* Figure E1 in the online supplement).

Deregulation of matriptase activity often relates to an imbalance with its endogenous inhibitor HAI-1. Hence, we determined the HAI-1 mRNA levels by qPCR and determined the ratio of matriptase/HAI-1 mRNA expression in control versus IPF lungs, as previously described (23). In IPF tissues, we observed a 1.2-fold increase in HAI-1 mRNA, and the ratio matriptase/HAI-1 was slightly up-regulated in patients with IPF (Table 1).

Next, we examined the cellular distribution of matriptase in lung biopsies of patients with IPF. Immunohistochemical staining showed prominent matriptase immunoreactivity in macrophages and epithelial cells overlying fibroblast foci and a weaker staining in (myo)fibroblasts of these foci (Figures 1D–1I). Endothelium staining was even weaker (not shown). In contrast, only sparse staining of AECs and monocytes was observed in the nonfibrotic part of the lungs of these patients (Figure 1J). There was no detectable signal for similar sections stained with an isotype-specific control antibody (Figure 1K). Finally, using primary IPF AEC and fibroblasts derived from a different (German) cohort, we assessed the relative expression of matriptase by qPCR and confirmed that matriptase mRNA level is higher in fibrotic AECs and weaker in fibrotic fibroblasts (Figure 1L).

Modulation of Matriptase Expression *In Vitro* in Pulmonary Cells

We next analyzed the modulation of matriptase expression in pulmonary cells. Western blots of primary human pulmonary fibroblasts derived from IPF tissues (Figure 2A) showed 1.7 ± 0.4-fold higher matriptase expression (*lanes 6–9*) than from control fibroblasts (*lanes 1–5*). Because transforming growth factor (TGF)-β is a master switch in the development of fibrosis during IPF (24), we also assessed its action on pulmonary cells. Stimulation of control (*lanes 10–14*) or fibrotic (*lanes 15–18*) fibroblasts for 48 hours by TGF-β (1 ng/ml) robustly enhanced matriptase expression by 3.1 ± 0.5- and 5.1 ± 1.5-fold, respectively (Figure 2A). Consistent with previous

Figure 1. (Continued). (*lanes 1–6*) or patients (IPF, *lanes 8–13*). *Lane 7*: molecular marker. Tubulin serves as loading control. (*Bottom*) Densitometry values for matriptase and PAR-2 were normalized to tubulin. Values were expressed as fold increase over control (*open bars*) and are shown in the bar graph. $^{*}P < 0.05$. (*C*) The relative proteolytic activity of matriptase was determined in IPF (n = 28) and control (n = 26). For each group, the different tissue homogenates were incubated with 100 μM of the matriptase highly selective fluorogenic substrate t-butyloxycarbonyl Boc-Gln-Ala-Arg-MCA (Boc-QAR-AMC), and the fluorogenic release was monitored at 300 minutes. Results presented as mean ± SEM are expressed as percentage of fluorescence in control tissues and are representative of two independent experiments. $^{****}P < 0.0001$. (*D–F*, *J*) Immunohistochemical matriptase staining of fibrotic (*D–F*) or nonfibrotic (*J*) regions of the lung of patients with IPF, showing enhanced matriptase expression in macrophages and interstitial mononuclear cells (*arrows*), epithelial cells (*arrowhead*), overlying a fibroblast focus (*FF*) (*E*, *inset* and *F*, ×200) and in (myo)fibroblasts of this focus (*asterisks*). (*G–I*) Representative serial lung sections from the same patients with IPF stained for α-smooth muscle actin (*G*), CD45 (*H*), and ABCA3 (*I*) staining of the same region. (*K*) Matriptase isotype control staining. (*L*) The relative mRNA levels of matriptase were assessed in IPF type II alveolar epithelial cells (AECII) (n = 7) and IPF fibroblasts (n = 4) by quantitative reverse transcriptase–polymerase chain reaction. Results are presented as mean ± SEM ΔCt (matriptase−HPRT). $^{**}P < 0.005$. HPRT = hypoxanthine-guanine phosphoribosyltransferase.

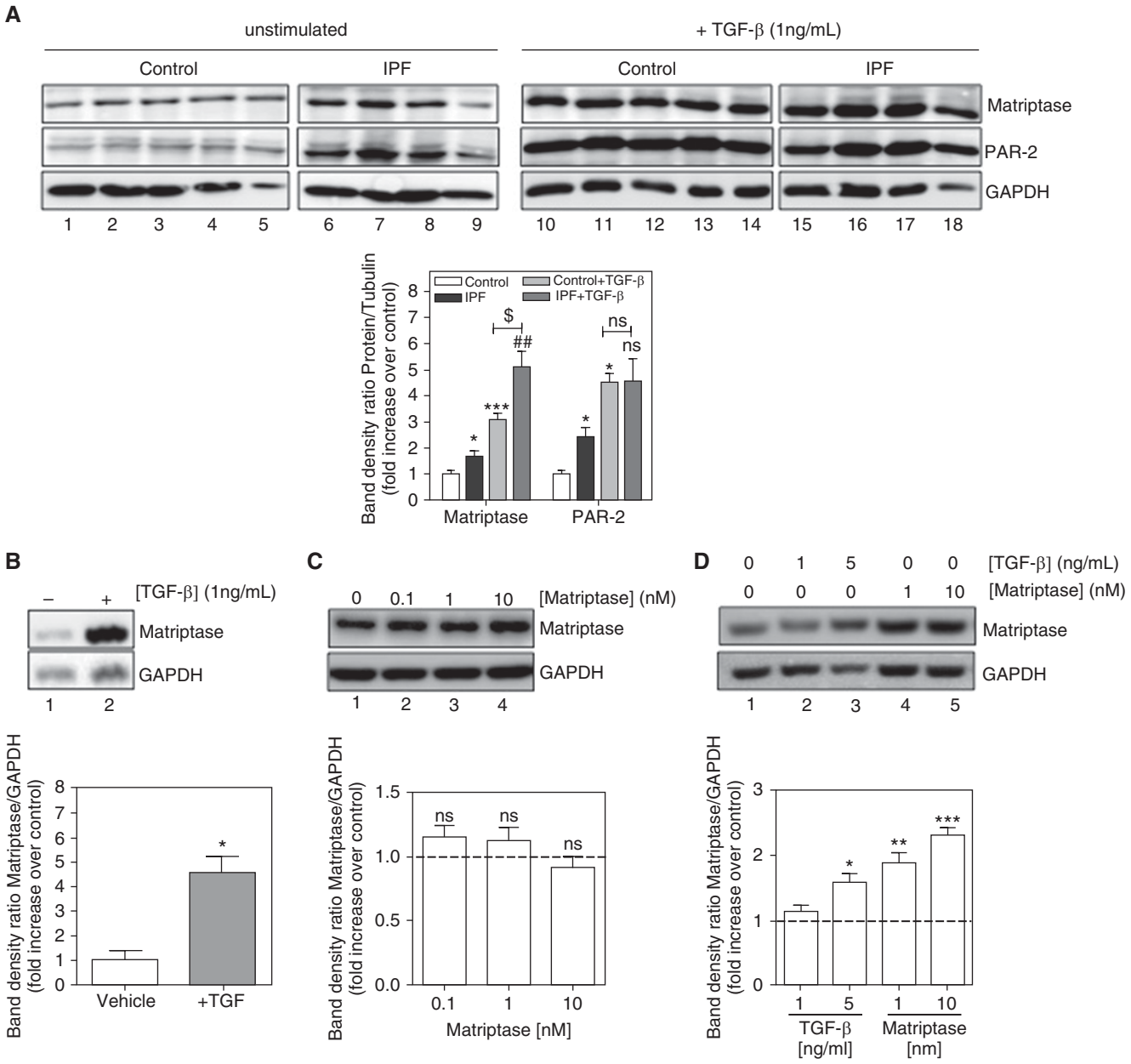

Figure 2. Differential modulation of matriptase expression in pulmonary cells. (*A*) (*Top*) Western blot analysis of matriptase and protease-activated receptor-2 (PAR-2) expression in primary fibroblasts derived from control (*lanes 1–5* and *10–14*) or idiopathic pulmonary fibrosis (IPF) (*lanes 6–9* and *15–18*), in the indicated conditions (respectively, unstimulated, *lanes 1–9*; or stimulated for 48 h with 1 ng/ml transforming growth factor [TGF]-β, *lanes 10–18*). (*Bottom*) Densitometry values were normalized to glyceraldehyde phosphate dehydrogenase (GAPDH). Values were expressed as fold changes over control (as indicated in the text) and are shown in the bar graph. $^{*}P < 0.05$, $^{***}P < 0.001$ compared with control (*white bars*), $^{\#\#}P < 0.005$ compared with IPF (*black bars*), $^{\$}P < 0.05$, ns = not significant. (*B*) (*Top*) Matriptase immunoblot on cell lysate of normal human lung fibroblasts showing that TGF-β treatment robustly drives matriptase expression (*lane 2*) compared with phosphate-buffered saline (PBS)-treated cells (*lane 1*). (*Bottom*) Densitometry values were normalized to GAPDH. Values were expressed as fold increases over control and are shown in the bar graph. $^{*}P < 0.05$. (*C*) (*Top*) Effect of different concentrations of matriptase on its own expression in primary control fibroblasts. Cells were stimulated for 48 hours with PBS (*lane 1*) or matriptase (*lanes 2–4*). (*Bottom*) The levels of matriptase in each experiment were normalized to GAPDH. Values of all treated samples were then normalized to that of a vehicle-treated sample that was set to 1 (*dashed line*). ns = not significant. (*D*) (*Top*) Western blot analysis of A549 cell lysate showing the effects of PBS (*lane 1*), 1–5 ng/ml TGF-β (*lanes 2–3*) or 1–10 nM matriptase (*lanes 4–5*) on matriptase expression. (*Bottom*) Densitometry values after normalization to GAPDH, shown as fold change over vehicle-treated cells (*dashed line*). $^{*}P < 0.05$, $^{**}P < 0.005$, $^{***}P < 0.001$ compared to control (*dashed line*). (*A–D*) GAPDH serves as a loading control. TGF-β = transforming growth factor-β.

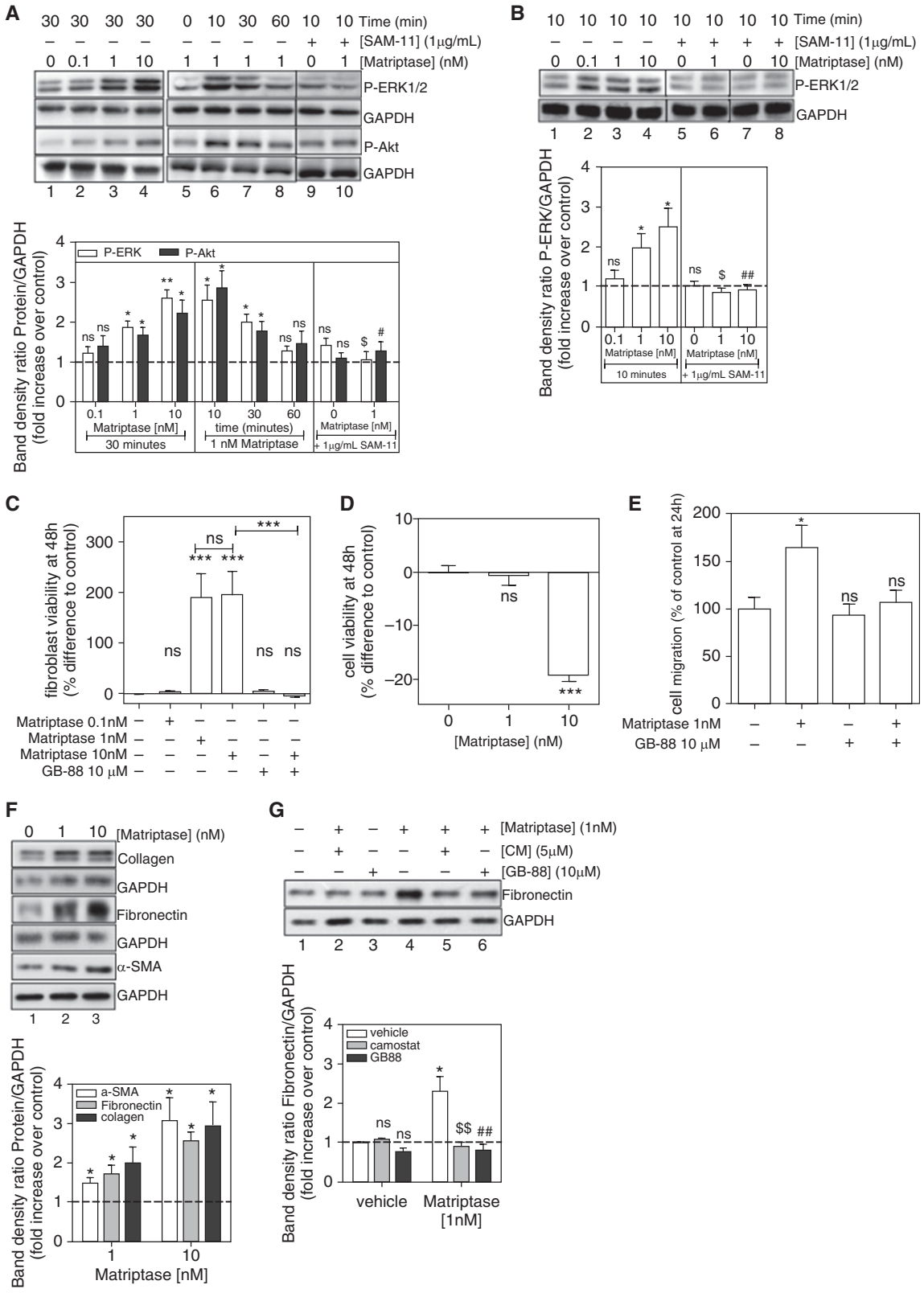

Figure 3. Matriptase signals to pulmonary cells via protease-activated receptor-2 (PAR-2) activation and triggers fibroproliferative responses. (*A*) (*Top*) Matriptase-induced phosphorylation of extracellular signal–regulated kinases 1/2 (ERK1/2) and v-akt murine thymoma viral oncogene (Akt) in fibroblasts is mediated by PAR-2. Serum-starved control pulmonary fibroblasts were treated with phosphate-buffered saline (PBS) (*lane 1*), 0.1–10 nM of matriptase for 30 minutes (*lanes 2–4*), or 1 nM matriptase for 0–60 minutes (*lanes 5–8*). *Lanes 9–10*, fibroblasts were preincubated for 30 minutes

studies (20, 21), PAR-2 was up-regulated in IPF and TGF-β–stimulated control fibroblasts (by 2.4 ± 0.8- and 4.5 ± 0.8-fold, respectively). To our knowledge, the action of TGF-β on PAR-2 expression in IPF fibroblasts has never been assessed. We observed in TGF-β–stimulated IPF fibroblasts that PAR-2 expression was unchanged ($P = 0.057$) (Figure 2A). The effects of TGF-β on matriptase expression were also examined in epithelial pulmonary cells and in normal human lung fibroblasts (NHLF). TGF-β induced matriptase up-regulation by 4.5 ± 1-fold in NHLF (Figure 2B) and by 1.6 ± 0.3-fold in epithelial pulmonary cells (Figure 2D, *lanes 1–3*). We also assessed the effects of matriptase on its own expression. We observed that, although 48-hour stimulation with 0 to 10 nM recombinant matriptase (which displays a potent activity similar to endogenous matriptase [7]) had no effect on fibroblasts (Figure 2C), matriptase efficiently up-regulated its own expression in epithelial pulmonary cells at 1 and 10 nM (by 1.9 ± 0.3- and 2.3 ± 0.2-fold, respectively) (Figure 2D, *lanes 4–5*).

Matriptase Evokes Fibroproliferative Responses *In Vitro* via PAR-2 Activation

We next characterized the signaling elicited by matriptase in pulmonary cells. Control fibroblasts were stimulated for 30 minutes with 0 to 10 nM matriptase or for 0 to 60 minutes with 1 nM matriptase. We analyzed the phosphorylation of extracellular signal–regulated kinases 1/2 (ERK1/2) and v-akt murine thymoma viral oncogene (AKT), which mediate influential signaling pathways in pulmonary fibrogenesis (25). Figure 3A shows that matriptase stimulated a time- and dose-dependent phosphorylation of both kinases. Furthermore, to determine whether PAR-2 mediates matriptase-induced signaling, cells were preincubated for 30 minutes with the PAR-2 blocking antibody, SAM-11 (26, 27), and subsequently stimulated for 10 min with 1 nM matriptase. Pretreatment with SAM-11 strongly reduced the matriptase-induced phosphorylation of ERK1/2 or Akt (Figure 3A). Similar results were obtained with epithelial pulmonary cells (Figure 3B) and NHLF (not shown). Altogether, these data demonstrate that matriptase signals to pulmonary cells via PAR-2 activation.

The effects of 48-hour incubation with 0 to 10 nM matriptase on cell proliferation were also assessed by a WST-1 assay. As shown in Figure 3C, 1 nM and 10 nM matriptase significantly enhanced control fibroblast proliferation by 188 ± 134% and 239 ± 79%, respectively. Similar results were obtained with NHLF. Furthermore, matriptase-induced cell survival was PAR-2 dependent, as pretreatment with 10 μM GB88, a specific PAR-2 antagonist (28), abolished the effect of 10 nM matriptase on fibroblast proliferation. Strikingly, matriptase led to a dose-dependent decrease in epithelial pulmonary cell proliferation by 19.4 ± 1.1% (Figure 3D). We also analyzed the effects of matriptase on fibroblast migration in a modified Boyden chamber. As shown on Figure 3E, 1 nM matriptase enhanced cell migration by 175 ± 46%. This effect was reversed by 10 μM GB-88, underlying PAR-2 involvement in matriptase-mediated cell migration. We subsequently examined whether matriptase triggers fibroblast activation and stimulates extracellular matrix component synthesis. As shown in Figure 3F, 48-hour stimulation with 1 or 10 nM of matriptase promoted significant increases (1.5 ± 0.3- and 3.1 ± 1.2-fold) in α-smooth muscle actin (SMA), a hallmark for myofibroblast differentiation, as well as in production of collagen (1.6 ± 0.3- and 2.4 ± 0.6-fold) and fibronectin (by 1.9 ± 0.7- and 2.3 ± 0.7-fold). These responses were specific and PAR-2 dependent. Preincubation of the cells for 1 hour with 5 μM CM, a specific, potent matriptase inhibitor (29–31) that does not affect thrombin activity (Figure E3), or the PAR-2 antagonist GB88 (10 μM), reversed matriptase-induced protein expression (Figure 3G).

Overall, these data implicate a contributing role for matriptase in IPF

Figure 3. (Continued). with the PAR-2 blocking antibody SAM-11 and subsequently stimulated with PBS (*lane 9*) or 1 nM matriptase (*lane 10*). Glyceraldehyde phosphate dehydrogenase (GAPDH) serves as a loading control. (*Bottom*) Densitometry values for P-ERK (*open bars*) and P-Akt (*solid bars*) were normalized to GAPDH. Values were expressed as fold changes over vehicle-treated cells (*dashed line*) and are shown in the bar graph. ns = not significant. $^{*}P < 0.05$, $^{**}P < 0.005$, $^{\$}P < 0.05$ compared with P-ERK in the 1 nM matriptase condition; $^{\#}P < 0.05$ compared with P-Akt in the 1 nM matriptase condition, ns = not significant. (*B*) (*Top*) Matriptase also activates phospho-ERK1/2 in A549 cells via PAR-2 activation. Serum-starved A549 cells were stimulated either for 10 minutes with PBS (*lane 1*) or 0.1–10 nM matriptase (*lanes 2–4*), or with SAM-11 (*lanes 5–8*) and subsequently incubated for 10 minutes with 1 and 10 nM matriptase (*lanes 6 and 8*). GAPDH serves as a loading control. (*Bottom*) Densitometry values for P-ERK were normalized to GAPDH. Values were expressed as fold changes over vehicle-treated cells (*dashed line*) and are shown in the bar graph. ns = not significant. $^{*}P < 0.05$, $^{\$}P < 0.05$ compared with P-ERK in the 1 nM matriptase condition; $^{\#\#}P < 0.005$ compared with P-ERK in the 10 nM matriptase condition. (*C*) Matriptase enhances primary fibroblast survival via PAR-2 activation. Survival of control primary fibroblasts seeded in medium containing 1% fetal calf serum (FCS) and treated for 48 hours with PBS ([−], control condition) or the indicated concentrations of matriptase (+), in the presence (+) or in the absence (−) of the PAR-2 inhibitor GB-88. (*D*) Survival of A549 cells seeded in 1% FCS-containing medium, stimulated for 48 hours with PBS, 1 or 10 nM of matriptase. Results are shown as mean ± SEM of four (*C*) or three (*D*) independent experiments performed in sextuplicate. ns = not significant, $^{***}P < 0.001$. (*E*) Migration of normal human lung fibroblasts toward 1% FCS-containing medium (control), or medium supplemented with 1 nM matriptase, in the absence (−) or in the presence (+) of the PAR-2 antagonist GB-88. Results are shown as the mean ± SEM of five experiments. ns = not significant, $^{*}P < 0.05$. (*F*) (*Top*) Matriptase enhances the expression of α-smooth muscle actin (α-SMA), collagen, and fibronectin in control primary fibroblasts. Western blot analysis of serum-starved cells treated for 48 hours with PBS (*lane 1*), or 1 and 10 nM of matriptase (*lanes 2–3*). Shown are representative blots of experiments that were performed independently at least three times. GAPDH serves as a loading control. (*Bottom*) Densitometry values for α-SMA (*white bars*), collagen (*gray bars*), and fibronectin (*black bars*) were normalized to GAPDH. Values were expressed as fold changes over vehicle-treated cells (*dashed line*) and are shown in the bar graph. ns = not significant. $^{*}P < 0.05$. (*G*) (*Top*) Matriptase-induced protein synthesis is specific and PAR-2 dependent. Western blot analysis of fibronectin expression in serum-starved cells preincubated for 1 hour with PBS (*lane 1*), camostat mesilate (CM; *lane 2*), GB-88 (*lane 3*), and subsequently stimulated for 48 hours with 1 nM matriptase (*lanes 4–6*). Shown are representative blots of experiments that were performed independently at least three times. GAPDH serves as a loading control. (*Bottom*) Densitometry values for vehicle (*white bars*), CM (*gray bars*), and GB-88 (*black bars*), in the absence (−matriptase) or in the presence (+matriptase) of 1 nM matriptase, were normalized to GAPDH. Values were expressed as fold change over vehicle (*dashed line*) and are shown in the bar graph. ns = not significant. $^{*}P < 0.05$; $^{\$\$}P < 0.005$ and $^{\#}P < 0.05$ for 1 nM matriptase in the vehicle condition versus CM + matriptase and GB-88 + matriptase, respectively.

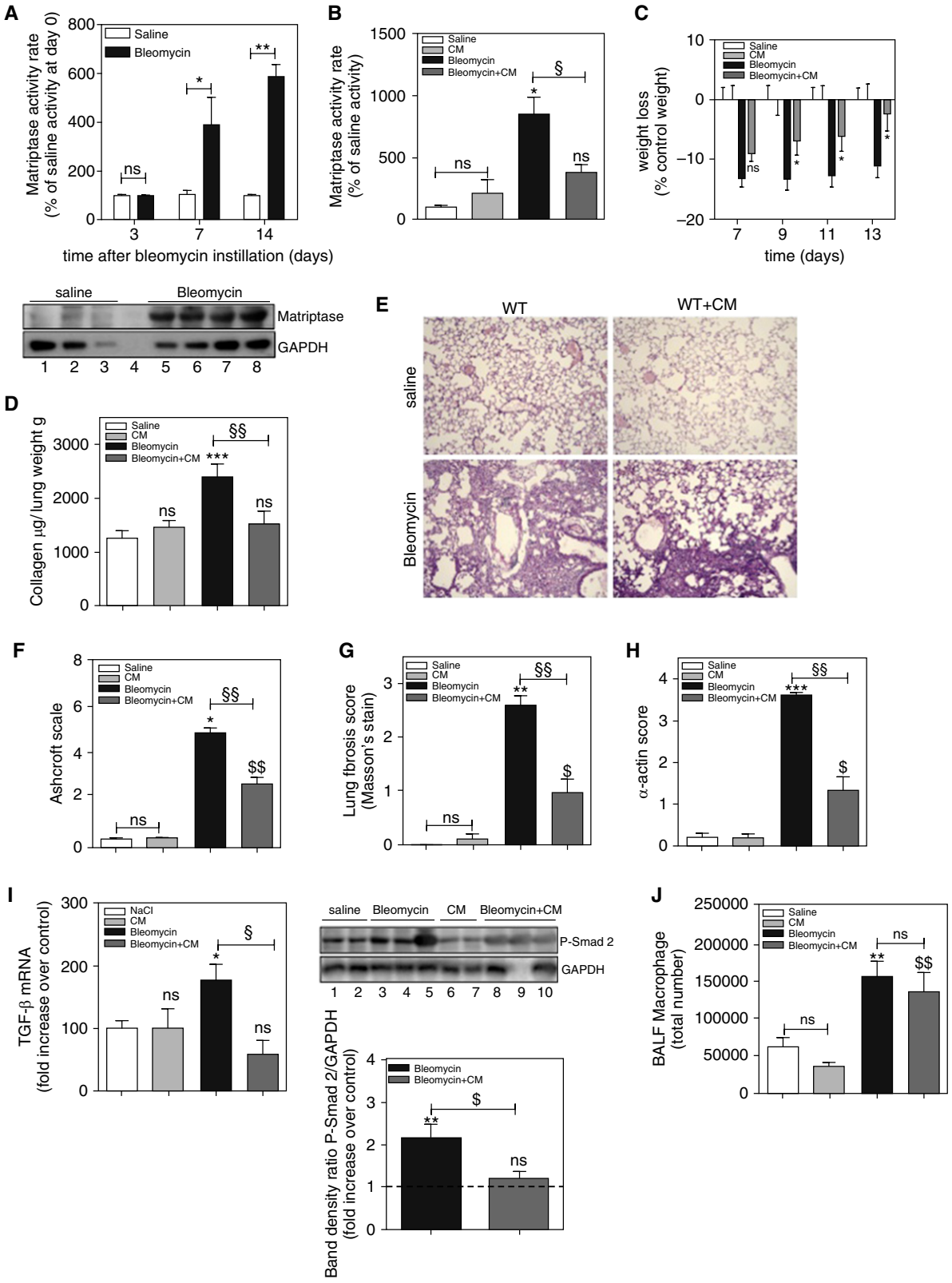

Figure 4. Matriptase inhibition by camostat mesilate (CM) affords protection from experimental bleomycin-induced pulmonary fibrosis. (*A*) (*Top*) Matriptase activity in murine lung homogenates, determined by the cleavage of the fluorogenic substrate Boc-QAR-AMC, 3, 7, and 14 days after saline (*open bars*; respectively, n = 3, n = 3, and n = 6 mice per group) or bleomycin instillation (*solid bars*; respectively, n = 3, n = 5, and n = 14 mice per group). Results are presented as mean ± SEM percentage of matriptase activity in the saline-treated mice at Day 3. ns = not significant, $^*P < 0.05$, $^{**}P < 0.005$.

pathogenesis, prompting us to further analyze the effects of modulating matriptase in experimental bleomycin-induced pulmonary fibrosis.

Matriptase Expression and Activity Are Increased during Experimental Pulmonary Fibrosis

Mice subjected to a single orotracheal instillation of bleomycin developed pulmonary fibrosis over a 2-week time course (inflammatory phase, Days 1–7; fibrosing phase, Days 7–14). Figure 4A shows data for the temporal modulation of matriptase expression and activity in murine lungs in this experimental model. Matriptase activity significantly increased by Day 7 (by 388 ± 114%) and Day 14 (by 587 ± 50%) (Figure 4A, *top panel*). Accordingly, immunoblotting confirmed an increase in pulmonary matriptase expression 14 days after bleomycin instillation (Figure 4A, *bottom panel*). Hence, we assessed the efficacy of the matriptase inhibitor CM, when administrated from Day 7 onward after the bleomycin challenge (delayed treatment), on pulmonary fibrosis development.

Inhibition of Matriptase by CM Attenuates Pulmonary Fibrogenesis *In Vivo*

CM is clinically used to treat pancreatitis. We initiated a delayed treatment by CM at the same dose range administered to patients (32). CM treatment significantly reduced matriptase activity in murine lung homogenates 14 days after bleomycin challenge (853 ± 130% to 381 ± 63%) (Figure 4B). Additionally, the loss in body weight (determined from Day 7 onward) in the bleomycin group was significantly attenuated in the CM-treated group (Figure 4C). We next quantified total pulmonary collagen content 14 days after bleomycin challenge. The collagen content strongly increased after bleomycin treatment (from 1,261 ± 463 to 2,408 ± 747 μg/g lung) and was blunted in the bleomycin + CM group (1,527 ± 664 μg/g lung) (Figure 4D). Accordingly, histologic assessment of the lung structure revealed that delayed CM treatment significantly attenuated the alveolar wall thickening due to inflammation and fibrosis (Figure 4E, *bottom panels*). The Ashcroft scoring system confirmed that CM treatment significantly reduced the severity of the lesions induced by bleomycin exposure (2.7 ± 0.3 vs. 4.9 ± 0.2, respectively) (Figure 4F). Accordingly, a reduced fibrosis score determined on semiquantitative assessment of Masson trichrome staining was observed in CM-treated animals (Figure 4G). A potential mechanism by which matriptase inhibition is protective could be by preventing myofibroblast differentiation. Indeed, semiquantitative assessment of α-SMA staining revealed a markedly reduced α-SMA expression in bleomycin + CM versus bleomycin groups (1.3 ± 0.7 vs. 3.61 ± 0.1, Figure 4H). We next assessed TGF-β expression and signaling. As shown in Figure 4I, TGF-β mRNA was strongly up-regulated on bleomycin challenge (by 177 ± 50%), whereas in the bleomycin + CM–treated group, it was significantly reduced. Accordingly, Smad-2 phosphorylation was significantly increased by bleomycin and was markedly attenuated by CM (respectively, 2.1 ± 0.7- vs. 1.2 ± 0.4-fold increase).

Figure 4. (Continued). (*Bottom*) Matriptase expression in murine lung homogenate 14 days after saline (*lanes 1–3*) or bleomycin (*lanes 5–8*) instillation. *Lane 4*: molecular marker. Glyceraldehyde phosphate dehydrogenase (GAPDH) serves as a loading control. (*B*) Matriptase activity in lung homogenate 14 days after saline (*white bar*, n = 4 mice), sham (CM only, *light gray bar*, n = 4 mice), bleomycin (*black bar*, n = 10 mice), or bleomycin + CM (*dark gray bar*, n = 7 mice) instillation. Results are presented as mean ± SEM percentage of matriptase activity in saline-treated mice. ns = not significant, $^{*}P < 0.05$ for bleomycin versus saline-treated mice, $^{\S}P < 0.05$ for bleomycin versus bleomycin + CM–treated mice. (*C*) Camostat mesilate treatment alleviates the weight loss induced by bleomycin. Depicted is the mean ± SEM percentage weight loss of the bleomycin- (*black bars*) or bleomycin + CM– (*dark gray bars*) treated mice (n = 18 animals per group), compared with their respective controls at the indicated time points. ns = not significant, $^{*}P < 0.05$ for bleomycin- versus bleomycin + CM–treated mice. (*D*) Collagen content in lung homogenate 14 days after saline (*white bar*, n = 12 mice), sham (CM only, *light gray bar*, n = 10 mice), bleomycin (*black bar*, n = 8 mice), or bleomycin + CM (*dark gray bar*, n = 9 mice) instillation. The collagen content, determined by Sircol assay, was adjusted for tissue weight. Results are expressed as means ± SEM; n = 8–12 mice per group. $^{***}P < 0.001$ for bleomycin versus saline-treated mice, $^{\S\S}P < 0.005$ for bleomycin versus bleomycin + CM–treated mice; ns = not significant. (*E*) Hematoxylin and eosin staining of lung tissue sections from saline-, sham- (wild type [WT] and WT + CM, *top left* and *top right panels*, respectively), bleomycin- and bleomycin + CM– (*bottom left* and *bottom right panels*, respectively) treated mice. (*F*) Assessment of the severity of pulmonary fibrosis on Ashcroft scale 14 days after saline (*white bar*), sham (CM only, *light gray bar*), bleomycin (*black bar*), or bleomycin + CM (*dark gray bar*) instillation. Depicted is the mean ± SEM histological score, n = 3–6 mice per group. ns = not significant, $^{*}P < 0.05$ for bleomycin versus saline-treated mice, $^{\$\$}P < 0.005$ for bleomycin + CM versus CM, $^{\S\S}P < 0.005$ for bleomycin- versus bleomycin + CM-treated mice. (*G*) Fibrosis scoring of the Masson trichrome staining 14 days after saline (*white bar*, n = 3 mice), sham (CM only, *light gray bar*, n = 5 mice), bleomycin (*black bar*, n = 6 mice), or bleomycin + CM (*dark gray bar*, n = 6 mice) instillation. Depicted is the mean ± SEM fibrosis score. ns = not significant, $^{**}P < 0.005$ for bleomycin versus saline-treated mice, $^{\S\S}P < 0.005$ for bleomycin versus bleomycin + CM–treated mice, $^{\$}P < 0.005$ for bleomycin + CM versus CM. (*H*) Semiquantitative scoring of α-actin staining after saline (*white bar*), sham (CM only, *light gray bar*), bleomycin (*black bar*), or bleomycin + CM (*dark gray bar*) instillation. Depicted is the mean ± SEM fibrosis score (n = 5–6 mice per group). ns = not significant, $^{***}P < 0.001$ for bleomycin- versus saline-treated mice, $^{\S\S}P < 0.005$ for bleomycin- versus bleomycin + CM–treated mice, $^{\$}P < 0.005$ for bleomycin + CM versus CM. (*I*) CM reduces transforming growth factor (TGF)-β expression and Smad 2 phosphorylation in fibrotic lung. (*Left panel*) mRNA expression of TGF-β in the different groups of mice. Expression of mRNA was normalized to β2-microglobulin. Values are expressed as the mean fold increase over saline group ± SEM (n = 4–6 mice per group). ns = not significant, $^{*}P < 0.05$ for bleomycin- versus saline-treated mice, $^{\S}P < 0.051$ for bleomycin- versus bleomycin + CM–treated mice. (*Right panel*, *top*) Representative Western blot analysis of Smad 2 phosphorylation in lung homogenates from mice treated with saline (*lanes 1–2*), CM only (*lanes 6–7*), bleomycin (*lanes 3–5*), and bleomycin + CM (*lanes 8–10*) 14 days after bleomycin instillation. GAPDH serves as a loading control. (*Right panel*, *bottom*) Densitometry analysis for Smad 2 phosphorylation (p-Smad 2). The *dashed line* represents the mean expression of p-Smad 2 in saline-treated mice. Data represent the mean ± SEM (n = 5–6 mice per group). $^{**}P < 0.005$ for bleomycin- versus saline-treated mice; $^{\$}P < 0.05$ for bleomycin + CM versus CM. ns = not significant. (*J*) CM treatment does not change the inflammatory response to bleomycin challenge. Data represent the mean ± SEM of macrophage count in the bronchoalveolar lavage fluid (BALF) after saline (*white bar*, n = 3 mice), sham (*light gray bar*, n = 4 mice), bleomycin (*black bar*, n = 9 mice) or bleomycin + CM (*dark gray bar*, n = 7 mice) treatment. $^{**}P < 0.005$ for bleomycin- versus saline-treated mice; $^{\$\$}P < 0.005$ for bleomycin + CM versus CM. ns = not significant.

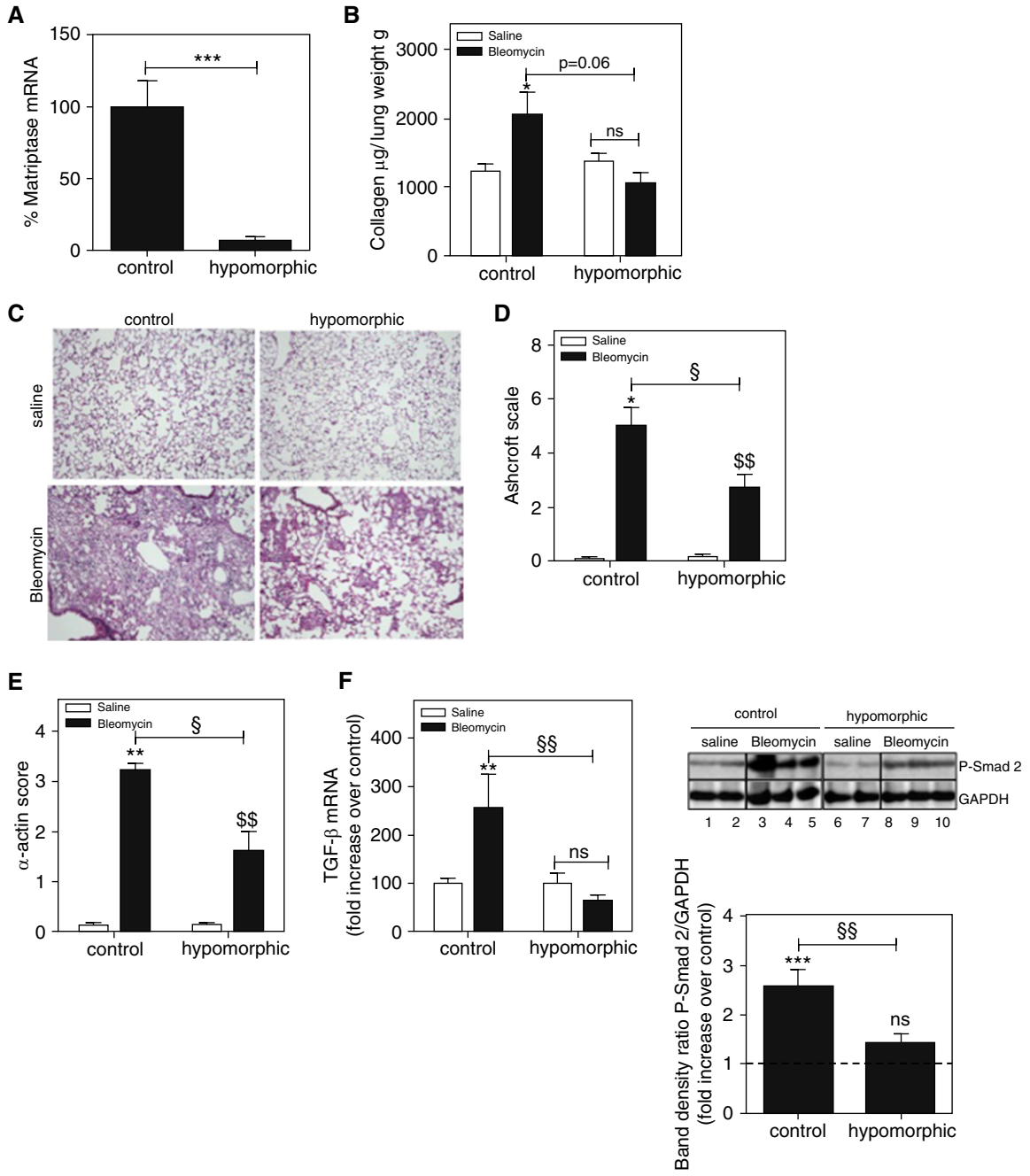

Figure 5. Matriptase hypomorphic mice are protected from experimental bleomycin-induced pulmonary fibrosis. (*A*) Matriptase mRNA levels in pulmonary tissue of matriptase hypomorphic mice (n = 10 mice) compared with control littermates (n = 7 mice) analyzed by quantitative polymerase chain reaction. Shown is mean ± SEM. $^{***}P < 0.001$. (*B*) Collagen content in lung homogenate 14 days after saline (*open bars*), or bleomycin (*solid bars*) instillation in control and matriptase hypomorphic mice. The collagen content, determined by Sircol assay, was adjusted for tissue weight. Results are expressed as mean ± SEM; n = 3–11 mice per group. $^{*}P < 0.05$ for bleomycin- versus saline-treated control mice. ns = not significant. (*C*) Hematoxylin and eosin staining of lung tissue sections of control or hypomorphic mice treated with saline (*top panels*) or bleomycin (*bottom panels*) for 14 days. (*D*) Assessment of the severity of pulmonary fibrosis on Ashcroft scale 14 days after saline (*open bars*), or bleomycin (*solid bars*) instillation. Depicted is the mean ± SEM histological score, n = 3–9 mice per group. $^{*}P < 0.05$ for bleomycin- versus saline-treated control mice, $^{\S}P < 0.05$ for bleomycin-treated control mice versus bleomycin-treated hypomorphic mice, $^{\$\$}P < 0.005$ for bleomycin- versus saline-treated hypomorphic mice. (*E*) Semiquantitative scoring of α-actin staining after saline (*open bars*), or bleomycin (*solid bars*) instillation in control and hypomorphic mice. Depicted is the mean ± SEM fibrosis score, n = 3–11 mice per group. $^{**}P < 0.005$ for bleomycin- versus saline-treated mice, $^{\S}P < 0.05$ for bleomycin-treated control mice versus bleomycin-treated hypomorphic mice, $^{\$\$}P < 0.005$ for bleomycin- versus saline-treated hypomorphic mice. (*F*) Matriptase genetic down-regulation is associated with reduced transforming growth factor (TGF)-β expression and Smad 2 phosphorylation. (*Left panel*) mRNA expression of TGF-β in matriptase hypomorphic and control littermates. Expression of mRNA was normalized to β2-microglobulin. Values are expressed as the mean fold increase over saline

Finally, we determined the effects of CM on the inflammatory response. The total number of macrophages in bronchoalveolar lavage fluid was increased by bleomycin but remained unchanged in the CM-treated group (Figure 4J). The levels of the cytokines tumor necrosis factor-α, IL-6, and monocyte chemoattractant protein-1 were also unaffected by CM treatment (data not shown). Thus, CM does not seem to modulate the inflammatory responses. Altogether, these data suggest that CM treatment affords protection from bleomycin-induced pulmonary fibrosis, with the prevailing mechanisms seeming to be antifibrotic rather than antiinflammatory.

Consequences of Matriptase Genetic Down-regulation in Experimental Pulmonary Fibrogenesis

Finally, we assessed the effects of genetic matriptase depletion in pulmonary fibrosis. Matriptase deficiency is lethal (33). Hence, we used matriptase hypomorphic mice, which express low levels of pulmonary matriptase (17). Indeed, we observed that matriptase hypomorphic mice expressed 7.1 ± 6% of the matriptase mRNA levels detected in lung tissues of littermate control mice (Figure 5A). Matriptase hypomorphic mice and control mice were subjected to bleomycin-induced pulmonary fibrosis and killed 14 days after bleomycin challenge. Quantification of total pulmonary collagen content in control mice revealed that collagen was significantly increased after bleomycin treatment (from 1,232 ± 342 to 2,049 ± 569 μg/g lung). Interestingly, in the hypomorphic mice, there was no significant difference in collagen content between the saline- or bleomycin-treated groups (1,369 ± 286 vs. 1,070 ± 462 μg/g lung) (Figure 5B). Histologic assessment of the lung structure revealed that in matriptase hypomorphic mice, bleomycin-induced lung injury was reduced compared with the control mice (Figure 5C). Indeed, the severity of the lesions was reduced on the Ashcroft scale (2.7 ± 1 vs. 5 ± 1, respectively; Figure 5D). Quantitative assessment of α-SMA staining demonstrated that, after bleomycin treatment, α-SMA expression was significantly reduced in matriptase hypomorphic mice compared with control mice (Figure 5E). Finally, analysis of TGF-β expression and signaling in the two groups of mice revealed that, again, bleomycin elicited a significant increase of TGF-β mRNA in the control mice. In matriptase hypomorphic mice, there was no significant difference between saline and bleomycin groups. Accordingly, Smad-2 phosphorylation was increased by bleomycin in control mice but not in hypomorphic mice (respectively, by 2.5 ± 0.8 vs. 1.4 ± 0.5-fold; Figure 5F)

Hence, genetic matriptase down-regulation inhibits the bleomycin-induced collagen secretion, lung injury, and α-SMA expression with an efficiency comparable to that of pharmacological inhibition with CM.

Discussion

The present study establishes for the first time a link between the membrane-anchored serine protease matriptase and IPF. Increased matriptase expression and activity were detected in human IPF specimens compared with controls. *In vitro*, we observed in pulmonary cells a remarkable plasticity in matriptase expression in response to TGF-β. Of note, the fibroblastic modulation of PAR-2 is akin to that observed for matriptase. PAR-2 is a major matriptase substrate (6) and is involved in IPF (12, 21, 34, 35). Indeed, we observed that matriptase triggers key features involved in IPF via PAR-2 activation. Strikingly, matriptase orchestrates fibroblast activation (characterized by proliferation, migration, differentiation, and protein synthesis) while it contributes to pulmonary epithelial cell loss. Because membrane anchorage enables matriptase to interact with vicinal proteins on the same cell surface or on neighbor cells, it may be hypothesized that epithelial and/or fibroblastic matriptase contribute to the aberrant epithelial–mesenchymal crosstalk characterizing IPF, eventually leading to sustained pathological wound-healing response. Accordingly, in our experimental model of bleomycin-induced pulmonary fibrosis, matriptase genetic down-regulation effectively limits fibrosis development, collagen deposition, myofibroblast activation, and TGF-β expression and signaling, thereby establishing a causal role for matriptase in pulmonary fibrosis pathogenesis.

We showed that, similar to the results obtained with matriptase hypomorphic mice, delayed CM treatment (i.e., initiated after the inflammatory phase of the model, 7 days after the bleomycin challenge) substantially reduces pulmonary fibrosis. CM has successfully been used in experimental models of liver, pancreatic, and renal fibrosis (36–38), and the antifibrogenic effects of CM were attributable (at least partly) to reduced TGF-β expression and signaling. So far, CM efficiency had never been assessed in pulmonary fibrosis, and our results are consistent with these findings. CM has a relatively narrow inhibition spectrum among serine proteases. Indeed, besides matriptase, it displays a very high specificity for trypsin, and, to a lower extent, prostasin (29, 31), the expressions of which were unchanged in IPF lungs (data not shown). Because CM is already used in clinics, its safety and tolerance are well established (31, 32). All these advantages would be particularly favorable for long-term treatment in patients with IPF.

Several issues are relevant to interpreting these data. First, one might hypothesize that the CM effects may be mediated through thrombin inhibition. However, we demonstrated comparable antifibrotic effects of genetic and pharmacological matriptase depletion. Furthermore, *in vitro,* thrombin activity

Figure 5. (Continued). group ± SEM (n = 5–18 mice per group). ns = not significant, $^{**}P < 0.005$ for bleomycin- versus saline-treated mice, $^{§§}P < 0.005$ for bleomycin-treated control mice versus bleomycin-treated hypomorphic mice. (*Right panel, top*) Representative Western blot analysis of Smad 2 phosphorylation in lung homogenates from control (*lanes 1–5*) and matriptase hypomorphic (*lanes 6–10*) mice treated with saline (*lanes 1–2* and *6–7*), or bleomycin (*lanes 3–5* and *8–10*) for 14 days. Glyceraldehyde phosphate dehydrogenase (GAPDH) serves as a loading control. (*Right panel, bottom*) Densitometry analysis for Smad 2 phosphorylation (p-Smad 2). The *dashed line* represents the mean expression of p-Smad 2 in saline-treated mice. Data represent the mean ± SEM (n = 6–9 mice per group). $^{***}P < 0.001$ for bleomycin- versus saline-treated control mice; $^{§§}P < 0.005$ for bleomycin-treated control mice versus bleomycin-treated hypomorphic mice; ns = not significant.

is unaffected by a dose of CM that completely inhibits matriptase activity (Figure E3). Nevertheless, a possible involvement of other unknown serine protease(s) that is/are inhibited by CM in the pathogenesis of IPF cannot be excluded. Second, the antifibrotic effects of CM might be due to direct bleomycin inhibition. However, CM treatment in the present study was delayed and so is unlikely to interfere with the course of events triggered by bleomycin immediately after its delivery. Moreover, CM is efficient in the abovementioned experimental models of fibrosis affecting other organs, where fibrosis was induced by the administration of different agents (36, 37, 39, 40), surgical procedures (38, 41), or even spontaneously (42). Third, the collagen content might be overestimated in the Sircol assay (43). However, the data are consistent with Ashcroft, Masson trichrome, and α-SMA scoring in the different experimental conditions.

In the present study, matriptase was up-regulated by ~1.56-fold in IPF. Interestingly, another study demonstrated that, in mice, a modest overexpression (1.2- to 1.4-fold) of matriptase in the skin was sufficient to cause spontaneous squamous cell carcinoma in the absence of other environmental or genetic challenges and dramatically potentiated carcinogen-induced tumor formation. Regulation of matriptase activity by HAI-1 overexpression negated the oncogenic effects of matriptase (44). These observations are consistent with the results of our study. We find that a modest increase in matriptase expression and activity is associated with pulmonary fibrogenesis, and matriptase depletion, either using CM or genetic down-regulation, ablates this phenotype. Additionally, the reported matriptase-induced malignant conversion was preceded by progressive dermal hyperplasia and fibrosis, observations that are striking in the context of IPF. Indeed, the incidence of lung cancer in patients with IPF is higher than the general population (45). Thus, it is tempting to speculate that a modest overexpression of matriptase in human lung contributes to higher tumor susceptibility, but the identification of the specific molecular events that enable matriptase-induced transformation in the lung remains a substantial challenge.

To our knowledge, this is the first report for matriptase expression and modulation during pathogenesis in human pulmonary fibroblasts. Noteworthy, in the fibroblastic foci of IPF lungs, fibroblast staining for matriptase was weaker than in overlying epithelium. Moreover, in line with heterogeneity of the fibroblast population (46), not all fibroblasts were positive for matriptase. Nevertheless, our *in vitro* data confirmed that matriptase expression is increased in primary IPF fibroblasts compared with controls and is strongly driven by TGF-β in control fibroblasts. Obviously, TGF-β is not the sole cytokine contributing to fibrogenesis, and multiple factors and pathways involved in IPF pathogenesis (47) may also impact matriptase expression. Although matriptase expression and functions were initially ascribed to epithelial cells, recent studies demonstrated that matriptase is expressed in diverse cell types, including normal and malignant mesenchymal cells (48–52). Together with the present study, this shows the remarkable plasticity of matriptase in response to different stimuli, raising important new questions. It would be important to determine whether matriptase is salient in other diffuse parenchymal lung diseases, where CM might also be effective. The role of matriptase on AEC type II cells is obviously of interest in these future studies. Furthermore, CM is efficient in experimental models of fibrosis affecting other organs where PAR-2 is instrumental (40, 53, 54). Thus, further studies aimed at elucidating the role of matriptase in these diseases are warranted.

In conclusion, our results reveal a new role for matriptase in IPF and indicate that targeting matriptase, or treatment by CM, which is already in clinical use for other diseases, may represent potential therapies for the treatment of IPF. ■

Author disclosures are available with the text of this article at www.atsjournals.org.

References

1. King TE Jr, Pardo A, Selman M. Idiopathic pulmonary fibrosis. *Lancet* 2011;378:1949–1961.
2. King TE Jr, Bradford WZ, Castro-Bernardini S, Fagan EA, Glaspole I, Glassberg MK, Gorina E, Hopkins PM, Kardatzke D, Lancaster L, *et al*.; ASCEND Study Group. A phase 3 trial of pirfenidone in patients with idiopathic pulmonary fibrosis. *N Engl J Med* 2014; 370:2083–2092.
3. Richeldi L, du Bois RM, Raghu G, Azuma A, Brown KK, Costabel U, Cottin V, Flaherty KR, Hansell DM, Inoue Y, *et al*.; INPULSIS Trial Investigators. Efficacy and safety of nintedanib in idiopathic pulmonary fibrosis. *N Engl J Med* 2014;370:2071–2082.
4. Taillé C, Grootenboer-Mignot S, Boursier C, Michel L, Debray MP, Fagart J, Barrientos L, Mailleux A, Cigna N, Tubach F, *et al*. Identification of periplakin as a new target for autoreactivity in idiopathic pulmonary fibrosis. *Am J Respir Crit Care Med* 2011;183:759–766.
5. Wuyts WA, Antoniou KM, Borensztajn K, Costabel U, Cottin V, Crestani B, Grutters JC, Maher TM, Poletti V, Richeldi L, *et al*. Combination therapy: the future of management for idiopathic pulmonary fibrosis? *Lancet Respir Med* 2014;2:933–942.
6. Szabo R, Bugge TH. Membrane-anchored serine proteases in vertebrate cell and developmental biology. *Annu Rev Cell Dev Biol* 2011;27: 213–235.
7. Sales KU, Masedunskas A, Bey AL, Rasmussen AL, Weigert R, List K, Szabo R, Overbeek PA, Bugge TH. Matriptase initiates activation of epidermal pro-kallikrein and disease onset in a mouse model of Netherton syndrome. *Nat Genet* 2010;42:676–683.
8. Szabo R, Rasmussen AL, Moyer AB, Kosa P, Schafer JM, Molinolo AA, Gutkind JS, Bugge TH. c-Met-induced epithelial carcinogenesis is initiated by the serine protease matriptase. *Oncogene* 2011;30: 2003–2016.
9. Sales KU, Friis S, Konkel JE, Godiksen S, Hatakeyama M, Hansen KK, Rogatto SR, Szabo R, Vogel LK, Chen W, *et al*. Non-hematopoietic PAR-2 is essential for matriptase-driven pre-malignant progression and potentiation of ras-mediated squamous cell carcinogenesis. *Oncogene* 2015;34:346–356.
10. Diegelmann RF, Evans MC. Wound healing: an overview of acute, fibrotic and delayed healing. *Front Biosci* 2004;9:283–289.
11. Wynn TA. Integrating mechanisms of pulmonary fibrosis. *J Exp Med* 2011;208:1339–1350.
12. Borensztajn K, Bresser P, van der Loos C, Bot I, van den Blink B, den Bakker MA, Daalhuisen J, Groot AP, Peppelenbosch MP, von der Thüsen JH, *et al*. Protease-activated receptor-2 induces myofibroblast differentiation and tissue factor up-regulation during bleomycin-induced lung injury: potential role in pulmonary fibrosis. *Am J Pathol* 2010;177:2753–2764.
13. Borensztajn K, Peppelenbosch MP, Spek CA. Factor Xa: at the crossroads between coagulation and signaling in physiology and disease. *Trends Mol Med* 2008;14:429–440.

14. Oberst MD, Singh B, Ozdemirli M, Dickson RB, Johnson MD, Lin CY. Characterization of matriptase expression in normal human tissues. *J Histochem Cytochem* 2003;51:1017–1025.
15. Marchand-Adam S, Fabre A, Mailleux AA, Marchal J, Quesnel C, Kataoka H, Aubier M, Dehoux M, Soler P, Crestani B. Defect of pro-hepatocyte growth factor activation by fibroblasts in idiopathic pulmonary fibrosis. *Am J Respir Crit Care Med* 2006; 174:58–66.
16. Melboucy-Belkhir S, Pradère P, Tadbiri S, Habib S, Bacrot A, Brayer S, Mari B, Besnard V, Mailleux A, Guenther A, *et al*. Forkhead Box F1 represses cell growth and inhibits COL1 and ARPC2 expression in lung fibroblasts in vitro. *Am J Physiol Lung Cell Mol Physiol* 2014; 307:L838–L847.
17. List K, Currie B, Scharschmidt TC, Szabo R, Shireman J, Molinolo A, Cravatt BF, Segre J, Bugge TH. Autosomal ichthyosis with hypotrichosis syndrome displays low matriptase proteolytic activity and is phenocopied in ST14 hypomorphic mice. *J Biol Chem* 2007; 282:36714–36723.
18. Buzza MS, Netzel-Arnett S, Shea-Donohue T, Zhao A, Lin CY, List K, Szabo R, Fasano A, Bugge TH, Antalis TM. Membrane-anchored serine protease matriptase regulates epithelial barrier formation and permeability in the intestine. *Proc Natl Acad Sci USA* 2010;107: 4200–4205.
19. Fabre A, Marchal-Sommé J, Marchand-Adam S, Quesnel C, Borie R, Dehoux M, Ruffié C, Callebert J, Launay JM, Hénin D, *et al*. Modulation of bleomycin-induced lung fibrosis by serotonin receptor antagonists in mice. *Eur Respir J* 2008;32:426–436.
20. Sokolova E, Grishina Z, Bühling F, Welte T, Reiser G. Protease-activated receptor-1 in human lung fibroblasts mediates a negative feedback downregulation via prostaglandin E2. *Am J Physiol Lung Cell Mol Physiol* 2005;288:L793–L802.
21. Wygrecka M, Kwapiszewska G, Jablonska E, von Gerlach S, Henneke I, Zakrzewicz D, Guenther A, Preissner KT, Markart P. Role of protease-activated receptor-2 in idiopathic pulmonary fibrosis. *Am J Respir Crit Care Med* 2011;183:1703–1714.
22. Lee SL, Dickson RB, Lin CY. Activation of hepatocyte growth factor and urokinase/plasminogen activator by matriptase, an epithelial membrane serine protease. *J Biol Chem* 2000;275: 36720–36725.
23. Vogel LK, Saebø M, Skjelbred CF, Abell K, Pedersen ED, Vogel U, Kure EH. The ratio of Matriptase/HAI-1 mRNA is higher in colorectal cancer adenomas and carcinomas than corresponding tissue from control individuals. *BMC Cancer* 2006;6:176.
24. Fernandez IE, Eickelberg O. The impact of TGF-β on lung fibrosis: from targeting to biomarkers. *Proc Am Thorac Soc* 2012; 9:111–116.
25. Stella GM, Inghilleri S, Pignochino Y, Zorzetto M, Oggionni T, Morbini P, Luisetti M. Activation of oncogenic pathways in idiopathic pulmonary fibrosis. *Transl Oncol* 2014;7:650–655.
26. Lin KW, Park J, Crews AL, Li Y, Adler KB. Protease-activated receptor-2 (PAR-2) is a weak enhancer of mucin secretion by human bronchial epithelial cells in vitro. *Int J Biochem Cell Biol* 2008;40: 1379–1388.
27. Koo BH, Chung KH, Hwang KC, Kim DS. Factor Xa induces mitogenesis of coronary artery smooth muscle cell via activation of PAR-2. *FEBS Lett* 2002;523:85–89.
28. Lohman RJ, Cotterell AJ, Barry GD, Liu L, Suen JY, Vesey DA, Fairlie DP. An antagonist of human protease activated receptor-2 attenuates PAR2 signaling, macrophage activation, mast cell degranulation, and collagen-induced arthritis in rats. *FASEB J* 2012; 26:2877–2887.
29. Coote K, Atherton-Watson HC, Sugar R, Young A, MacKenzie-Beevor A, Gosling M, Bhalay G, Bloomfield G, Dunstan A, Bridges RJ, *et al*. Camostat attenuates airway epithelial sodium channel function in vivo through the inhibition of a channel-activating protease. *J Pharmacol Exp Ther* 2009;329:764–774.
30. Yamasaki Y, Satomi S, Murai N, Tsuzuki S, Fushiki T. Inhibition of membrane-type serine protease 1/matriptase by natural and synthetic protease inhibitors. *J Nutr Sci Vitaminol (Tokyo)* 2003;49: 27–32.
31. Rowe SM, Reeves G, Hathorne H, Solomon GM, Abbi S, Renard D, Lock R, Zhou P, Danahay H, Clancy JP, *et al*. Reduced sodium transport with nasal administration of the prostasin inhibitor camostat in subjects with cystic fibrosis. *Chest* 2013;144:200–207.
32. Kitagawa M, Naruse S, Ishiguro H, Hayakawa T. Pharmaceutical development for treating pancreatic diseases. *Pancreas* 1998;16: 427–431.
33. List K, Haudenschild CC, Szabo R, Chen W, Wahl SM, Swaim W, Engelholm LH, Behrendt N, Bugge TH. Matriptase/MT-SP1 is required for postnatal survival, epidermal barrier function, hair follicle development, and thymic homeostasis. *Oncogene* 2002;21: 3765–3779.
34. Park YS, Park CM, Lee HJ, Goo JM, Chung DH, Lee SM, Yim JJ, Kim YW, Han SK, Yoo CG. Clinical implication of protease-activated receptor-2 in idiopathic pulmonary fibrosis. *Respir Med* 2013;107: 256–262.
35. Vasakova M, Sterclova M, Matej R, Olejar T, Kolesar L, Skibova J, Striz I. IL-4 polymorphisms, HRCT score and lung tissue markers in idiopathic pulmonary fibrosis. *Hum Immunol* 2013;74:1346–1351.
36. Okuno M, Akita K, Moriwaki H, Kawada N, Ikeda K, Kaneda K, Suzuki Y, Kojima S. Prevention of rat hepatic fibrosis by the protease inhibitor, camostat mesilate, via reduced generation of active TGF-beta. *Gastroenterology* 2001;120:1784–1800.
37. Gibo J, Ito T, Kawabe K, Hisano T, Inoue M, Fujimori N, Oono T, Arita Y, Nawata H. Camostat mesilate attenuates pancreatic fibrosis via inhibition of monocytes and pancreatic stellate cells activity. *Lab Invest* 2005;85:75–89.
38. Hayata M, Kakizoe Y, Uchimura K, Morinaga J, Yamazoe R, Mizumoto T, Onoue T, Ueda M, Shiraishi N, Adachi M, *et al*. Effect of a serine protease inhibitor on the progression of chronic renal failure. *Am J Physiol Renal Physiol* 2012;303:F1126–F1135.
39. Emori Y, Mizushima T, Matsumura N, Ochi K, Tanioka H, Shirahige A, Ichimura M, Shinji T, Koide N, Tanimoto M. Camostat, an oral trypsin inhibitor, reduces pancreatic fibrosis induced by repeated administration of a superoxide dismutase inhibitor in rats. *J Gastroenterol Hepatol* 2005;20:895–899.
40. Ishikura H, Nishimura S, Matsunami M, Tsujiuchi T, Ishiki T, Sekiguchi F, Naruse M, Nakatani T, Kamanaka Y, Kawabata A. The proteinase inhibitor camostat mesilate suppresses pancreatic pain in rodents. *Life Sci* 2007;80:1999–2004.
41. Morinaga J, Kakizoe Y, Miyoshi T, Onoue T, Ueda M, Mizumoto T, Yamazoe R, Uchimura K, Hayata M, Shiraishi N, *et al*. The antifibrotic effect of a serine protease inhibitor in the kidney. *Am J Physiol Renal Physiol* 2013;305:F173–F181.
42. Jia D, Taguchi M, Otsuki M. Preventive and therapeutic effects of the protease inhibitor camostat on pancreatic fibrosis and atrophy in CCK-1 receptor-deficient rats. *Pancreas* 2005;30:54–61.
43. Lareu RR, Zeugolis DI, Abu-Rub M, Pandit A, Raghunath M. Essential modification of the Sircol Collagen Assay for the accurate quantification of collagen content in complex protein solutions. *Acta Biomater* 2010;6:3146–3151.
44. List K, Szabo R, Molinolo A, Sriuranpong V, Redeye V, Murdock T, Burke B, Nielsen BS, Gutkind JS, Bugge TH. Deregulated matriptase causes ras-independent multistage carcinogenesis and promotes ras-mediated malignant transformation. *Genes Dev* 2005;19: 1934–1950.
45. Harris JM, Johnston ID, Rudd R, Taylor AJ, Cullinan P. Cryptogenic fibrosing alveolitis and lung cancer: the BTS study. *Thorax* 2010;65: 70–76.
46. Fries KM, Blieden T, Looney RJ, Sempowski GD, Silvera MR, Willis RA, Phipps RP. Evidence of fibroblast heterogeneity and the role of fibroblast subpopulations in fibrosis. *Clin Immunol Immunopathol* 1994;72:283–292.
47. Fernandez IE, Eickelberg O. New cellular and molecular mechanisms of lung injury and fibrosis in idiopathic pulmonary fibrosis. *Lancet* 2012; 380:680–688.
48. Seitz I, Hess S, Schulz H, Eckl R, Busch G, Montens HP, Brandl R, Seidl S, Schömig A, Ott I. Membrane-type serine protease-1/matriptase induces interleukin-6 and -8 in endothelial cells by activation of protease-activated receptor-2: potential implications in atherosclerosis. *Arterioscler Thromb Vasc Biol* 2007;27:769–775.

49. Georgy SR, Pagel CN, Ghasem-Zadeh A, Zebaze RM, Pike RN, Sims NA, Mackie EJ. Proteinase-activated receptor-2 is required for normal osteoblast and osteoclast differentiation during skeletal growth and repair. *Bone* 2012;50:704–712.
50. Mukai S, Yorita K, Kawagoe Y, Katayama Y, Nakahara K, Kamibeppu T, Sugie S, Tukino H, Kamoto T, Kataoka H. Matriptase and MET are prominently expressed at the site of bone metastasis in renal cell carcinoma: immunohistochemical analysis. *Hum Cell* 2015;28: 44–50.
51. Milner JM, Patel A, Davidson RK, Swingler TE, Desilets A, Young DA, Kelso EB, Donell ST, Cawston TE, Clark IM, *et al*. Matriptase is a novel initiator of cartilage matrix degradation in osteoarthritis. *Arthritis Rheum* 2010;62:1955–1966.
52. Barretina J, Caponigro G, Stransky N, Venkatesan K, Margolin AA, Kim S, Wilson CJ, Lehár J, Kryukov GV, Sonkin D, *et al*. The Cancer Cell Line Encyclopedia enables predictive modelling of anticancer drug sensitivity. *Nature* 2012;483:603–607.
53. Knight V, Tchongue J, Lourensz D, Tipping P, Sievert W. Protease-activated receptor 2 promotes experimental liver fibrosis in mice and activates human hepatic stellate cells. *Hepatology* 2012;55: 879–887.
54. Chung H, Ramachandran R, Hollenberg MD, Muruve DA. Proteinase-activated receptor-2 transactivation of epidermal growth factor receptor and transforming growth factor-β receptor signaling pathways contributes to renal fibrosis. *J Biol Chem* 2013;288: 37319–37331.